

Dynamic shear modulus of a semiflexible polymer network

F. Gittes and F. C. MacKintosh

Department of Physics and Biophysics Research Division, University of Michigan, Ann Arbor, Michigan 48109-1120

(Received 19 December 1997)

We construct a model for the dynamic shear modulus $G(\omega)$ of entangled or crosslinked networks of semiflexible polymer that can account for the high-frequency scaling behavior, $G(\omega) \sim \omega^{3/4}$, that has recently been observed in solutions of the biopolymer *F*-actin. As we argue, this behavior should not be unique to *F*-actin, but rather should be a clear characteristic of semiflexible polymers in general. We also report molecular dynamics simulations that support the single filament response that is the basis of our model for the network shear modulus. [S1063-651X(98)51908-3]

PACS number(s): 83.10.Nn, 83.50.Fc, 87.15.Da, 87.45.-k

Semiflexible polymers fit in a continuum of behavior that runs from flexible-chain systems (such as polystyrene) to rodlike solutions. Nevertheless, accepted models of flexible and rodlike polymers [1,2] do not seem to be adequate to describe the behavior of semiflexible systems, and as yet no well-established models for viscoelasticity in semiflexible networks exist. Perhaps one reason for this is that few synthetic polymers display a sufficiently large aspect ratio of persistence length ℓ_p (the e^{-1} decay length of angular correlation along the filament) to molecular diameter for the distinctive features of a semiflexible network to become apparent. Biopolymers, however, have proven to be excellent model systems in which to study semiflexible behavior because of their rather large molecular cross section: the protein *F*-actin (filamentous actin), with a diameter of about 5–7 nm, has a persistence length of 15–18 μm [3,4], while microtubules have diameters of 28 nm and persistence lengths of several millimeters [4]. Networks of *F*-actin can provide cells with mechanical stability while occupying a significantly smaller volume fraction of the cytosol than would be required for a flexible network. This is in part why semiflexible polymers have lately become the subject of much interest and debate. Recent theoretical and experimental studies of *F*-actin, in particular, have begun to resolve the unusual static and dynamic properties of semiflexible systems. Here, we describe a model that can account for the anomalous power-law increase of the shear modulus G , as $G(\omega) \propto \omega^{3/4}$, that has been observed recently in experiments on *F*-actin above a frequency of about 1 Hz [5,6]. We also show that this is a general signature of semiflexible polymer systems.

Our physical picture is as follows. A semiflexible polymer network is an isotropic, random array of long stiff chains that are subject to constraints (either steric entanglements or crosslinks) on a length scale ℓ_e shorter than the persistence length ℓ_p of the filaments. For our purposes, the defining characteristic of a semiflexible network is that the filaments are much longer than either the persistence length or the entanglement length: $L \gg \ell_p \gg \ell_e \gg a$, where L is the filament length and a is a molecular dimension. Under an applied macroscopic shear strain of frequency ω , filaments undergo a distortion that we assume to be affine above a length scale of order ℓ_e ; however, the precise value of this length will not be important for the high-frequency $G(\omega)$ as we

show below. A shear strain implies extension or compression in the fluctuating segments, depending on their orientation with respect to the shear direction. The longitudinal relaxation of the chain conformation through the surrounding viscous solvent results in a specific time-dependence of the response (microscopically, tension in the filament; macroscopically, stress in the solution) that is governed by the incompressibility of the filament along its contour length. It is this time-dependent, single filament response that results in a simple frequency dependence of the macroscopic stress response of the polymer network, in much the same way that the (single-filament) Rouse model describes the stress of both dilute and entangled flexible polymer solutions, and even of gels at high frequency. As such, this high-frequency response provides for a more quantitative comparison of experiment with theory than may be possible for the plateau modulus, which is highly sensitive to entanglement and crosslinking [7–10], and for which experimental values have varied widely [11].

For a strain $u_{ij} = \frac{1}{2}(\nabla_i u_j + \nabla_j u_i)$, a segment of orientation \hat{n} and length ℓ undergoes a relative change in end-to-end length of $\delta\ell/\ell = n_i n_j u_{ij}$, and there will be an induced tension τ_ω , given by $\delta\ell_\omega = \alpha_\omega \tau_\omega$, where $\alpha_\omega = \alpha'_\omega + i\alpha''_\omega$ is the longitudinal response function of the segment of filament. For a spatial density ρ of filaments, the stress due to filament tension is

$$\sigma_{ij}^{(\tau)} = \rho \langle \tau n_i n_j \rangle = \frac{\rho \ell_e}{\alpha_\omega} \langle n_i n_j n_k n_l \rangle u_{kl}. \quad (1)$$

There is an additional stress $-2i\omega\eta u_{ij}$ due to the solvent (with η the viscosity). For an isotropic distribution of filaments, $\langle n_i n_j n_k n_l \rangle = (1/15)\{\delta_{ij}\delta_{kl} + \delta_{ik}\delta_{jl} + \delta_{il}\delta_{jk}\}$. Assuming incompressibility ($u_{ii} = 0$) and identifying $\sigma_{ij} \equiv 2G(\omega)u_{ij}$, one finds

$$G(\omega) = \frac{1}{15} \rho \ell_e / \alpha_\omega - i\omega\eta. \quad (2)$$

In this way, at least for high frequencies, the macroscopic shear modulus of a network can be obtained from the single filament response.

We calculate the response function α_ω of a filament segment with length ℓ and bending modulus $\kappa = \ell_p kT$. The bending energy in the absence of tension is

$$U = \int_0^\ell ds \frac{\kappa}{2} (\partial^2 \mathbf{r}_\perp / \partial s^2)^2. \quad (3)$$

Writing the lateral deviation as $\mathbf{r}_\perp(s) = [u(s), v(s)]$, the tension-free equation for $u(s, t)$ is $\zeta \dot{u} = -\kappa \partial u / \partial s^4$, where ζ is the transverse drag coefficient. If the segment ends are laterally constrained, the motion is a sum of modes

$$u(s) = \frac{2}{\ell} \sum_q u_q \sin qs \quad (q = n\pi/\ell, n \geq 1), \quad (4)$$

and similarly for $v(s)$. Modes of differing q are uncorrelated. Denoting quantities at time $t > 0$ and at time 0 as primed and unprimed respectively, one finds

$$\langle u'_q u_q \rangle = \langle v'_q v_q \rangle = (\ell/2q^4 \ell_p) e^{-\omega_q t}, \quad (5)$$

where the relaxation rate is $\omega_q = (\kappa/\zeta)q^4$.

We defined α_ω as the response of a fluctuating segment of inextensible filament to a tension $\tau(t)$ [12]. A real filament, however, must possess some longitudinal compliance which will contribute to the response at very short times. We will discuss this restriction further below.

The total projected length change is given by

$$\delta \ell \approx -\frac{1}{2} \int_0^\ell ds (\partial \mathbf{r}_\perp / \partial s)^2 = -\frac{1}{\ell} \sum_q q^2 (u_q^2 + v_q^2). \quad (6)$$

Correlations of $\delta \ell$ evidently involve fourth-order correlations of u_q and v_q . However, since the energy [Eq. (3)] is quadratic in u and v , we can factor the fourth-order correlations using Wick's theorem: $\langle u_q'^2 u_q^2 \rangle = \langle u_q \rangle^2 + 2 \langle u_q' u_q \rangle^2$. The end-to-end correlation function $\phi(t) = \langle \delta \ell' \delta \ell \rangle - \langle \delta \ell \rangle^2$ is then easily found to be

$$\phi(t) = \frac{4}{\ell^2} \sum_q q^4 \langle u_q' u_q \rangle^2 = \frac{1}{\ell_p^2} \sum_q q^{-4} e^{-2\omega_q t}. \quad (7)$$

Transforming this correlation function and putting $q = n\pi/\ell$, we find the spectral density [13]

$$(\delta \ell^2)_\omega = \frac{1}{\omega_1 q_1^4 \ell_p^2} \sum_{n=1}^{\infty} \frac{1}{n^8 + (\omega/2\omega_1)^2}, \quad (8)$$

where $\omega_1 = (\kappa/\zeta)(\pi/\ell)^4$ is the relaxation rate of the slowest mode, $q = q_1 = \pi/\ell$. The imaginary part α''_ω of the response function is given by the fluctuation-dissipation theorem, $\alpha''_\omega = (\omega/2T)(\delta \ell^2)_\omega$, from which (choosing the poles to lie in the lower ω -plane for causality) we obtain the end-to-end response function of a segment of inextensible filament,

$$\alpha_\omega = \frac{1}{T q_1^4 \ell_p^2} \sum_{n=1}^{\infty} \frac{1}{n^4 - i\omega/2\omega_1}. \quad (9)$$

At low frequencies ($\omega \ll \omega_1$) Eq. (9) becomes $\alpha_{\text{plateau}} = (1/90)(\ell^4/T\ell_p^2)$. Using Eq. (2), and putting $\ell = \ell_e$, we find the plateau modulus of an entangled solution or the static modulus of a crosslinked gel: $G^{(0)} = 6\rho T \ell_p^2 / \ell_e^3$. This form of the plateau modulus agrees with a previous scaling result [7]. However, the physical validity of this $G^{(0)}$ is not

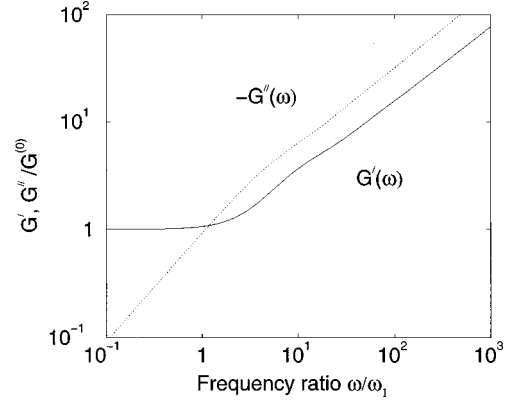


FIG. 1. Real part G' (solid line) and the absolute value $-G''$ of the imaginary part (dotted line) of the frequency-dependent shear modulus computed from Eq. (2), neglecting the term $-i\omega\eta$. G' and G'' are given relative to the plateau modulus $G^{(0)} = 6\rho T \ell_p^2 / \ell_e^3$, and the frequency is given in units of $2\omega_1$, where $\omega_1 = (\kappa/\zeta)(\pi/\ell_e)^4$. The plateau $G' = G^{(0)}$ extends to indefinitely low frequencies (as shown) only if the network is crosslinked.

clear from the present discussion; for example, if the network is not crosslinked, the filaments will slide past their entanglement points at low enough frequencies, and allow flow. The low-frequency regime is discussed in Refs. [14,9] and by Morse [10].

At high frequencies, we replace the sum in Eq. (9) by an integral to find

$$\alpha_\omega \approx \frac{1}{2\sqrt{2}} \frac{\ell}{T \ell_p^2} \left(\frac{2\kappa}{-i\zeta\omega} \right)^{3/4} \quad (\omega \gg \omega_1). \quad (10)$$

Again using Eq. (2), we find the shear modulus at high frequencies ($\omega \gg \omega_1$),

$$G(\omega) \approx \frac{1}{15} \rho \kappa \ell_p (-2i\zeta/\kappa)^{3/4} \omega^{3/4} - i\omega\eta. \quad (11)$$

We see that ℓ does not appear. Equation (9) displays a scaling regime of $G(\omega) \propto \omega^{3/4}$, up to an upper frequency ω_{visc} that is very sensitive to network density [15,16], $\omega_{\text{visc}} \propto \rho^4$. Above ω_{visc} , Eq. (9) crosses over to simple viscous scaling, $G(\omega) \propto \omega$. The $\omega^{3/4}$ scaling response depends solely on the density of filaments, their bending stiffness and their lateral drag coefficient ζ . It does not depend, for example, on network parameters such as the entanglement length ℓ_e . Filaments contribute independently to the shear modulus at high frequency, and there is no distinction between crosslinked networks and entangled solutions, as is also the case for flexible systems. For intermediate frequencies, Eq. (9) is in fact summable analytically; rather than evaluate that closed form, however, we perform the sum numerically: Fig. 1 shows the resulting real and imaginary parts of $G(\omega)$ that result via Eq. (2).

To test the predicted spectrum of end-to-end distance in Eq. (8), we performed a molecular dynamics simulation of an overdamped, semiflexible chain of twenty rigid segments which we defined to be of unit length. The drag coefficient of each vertex (equal to the drag per unit length) was taken to be $\zeta = 2T$. This choice determines the time step $\delta t = \varepsilon^2$, where ε^2 is the random variance of displacement for an un-

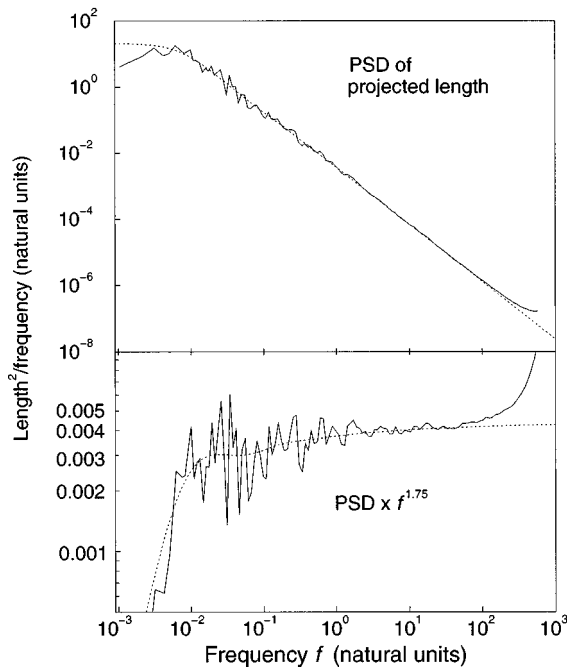


FIG. 2. Top: Power spectral density (solid line) of the projected end-to-end length of a fluctuating filament, with its ends constrained to lie on a fixed line. The persistence length is four times the filament length. Twenty inextensible segments of unit length were used to represent the filament. 3×2^{20} time steps were taken, with a step frequency of $f_s = 1.1 \times 10^3$. Equation (8) is shown for comparison (dotted line). There are no adjustable parameters. The final upturn is aliased diffusive power inherent in the discrete time steps. Bottom: The same curves multiplied by $f^{1.75}$; note the expanded scale. The limiting high-frequency power-law implicit in Eq. (8) would predict a horizontal line with value 0.0044.

constrained vertex. Finally, the elastic bending force on a vertex is $-\delta U / \delta \mathbf{r} = -\ell_p T \partial^4 \mathbf{r} / \partial n^4$, where U is given in Eq. (3). Here, because we are interested in the end-to-end distance fluctuations of a stiff filament, it was crucial to perform this simulation with strictly imposed arc length constraint. This required, at each time step, a random collective motion of the entire set of chain vertices within the constraint subspace [16]. The results of the dynamical calculation are shown in Fig. 2. We find good agreement, with no adjustable parameters, between the dynamics calculation and predictions of the model in Eq. (8).

We now ask how a small degree of longitudinal extensibility will change the foregoing results. For $\ell \ll \ell_p$, extensional dynamics and bending dynamics should occur independently. For a homogeneous elastic rod, extensional modes are described by $\zeta_{\parallel} \dot{x} = EA \partial^2 x / \partial s^2$, where $x(s)$ is the deformed longitudinal coordinate, ζ_{\parallel} is the longitudinal drag coefficient ($\zeta_{\parallel} \approx \zeta / 2$ [17,18]), E is Young's modulus, and A is the cross-sectional area. Longitudinal deformation propagates as

$$\delta x(s) \propto e^{(i-1)s/\ell_c}, \quad \ell_c = (2EA/\zeta_{\parallel}\omega)^{1/2}. \quad (12)$$

The length ℓ_c characterizes the decay of compressional effects at a frequency ω .

In actin filaments the compressional decay length ℓ_c is much larger than ℓ_p up to very high frequencies. With

straightforward modeling of the actin filaments as homogeneous cylinders [4], one estimates $EA \approx 5 \times 10^{-8}$ N, and a frequency of $f = 150$ kHz is needed to make ℓ_c as small as $10 \mu\text{m}$. Thus we can assume instantaneous tension propagation in F-actin up to very high frequencies. On length scales shorter than ℓ_c , we can put the static extensional response $\alpha^c = \ell / EA$ in parallel with the response function, Eq. (9). The latter is completely dominant out to frequencies of several MHz, so that extensional compliance is not relevant to experiments in F-actin.

Many of the parameters of our model have been measured for F-actin, which allows for quantitative comparison with experiment. Fluorescent, phalloidin-stabilized actin filaments have been estimated by observation of their thermal fluctuations [4] to have a persistence length of $\ell_p = \kappa / T = 17.7 \pm 1.1 \mu\text{m}$; other measurements have given similar results [3]. It is not known to what degree rigidity changes in the absence of phalloidin. The effective lateral drag coefficient of a filament includes a weak logarithmic dependence on the wavelength of motion, λ , or on some other large-scale cutoff to the hydrodynamics, such as mesh size. We arbitrarily fix this length scale at $\lambda \sim 1 \mu\text{m}$. Using the diameter of the filament ($d \approx 5$ nm for actin), we have $\zeta \approx 4\pi\eta / \ln(0.6\lambda/d) \approx 0.0023$ Ns/m² [18]. Using this drag coefficient, $\omega_q = (\kappa/\zeta)q^4$ implies a decay rate of 5 sec^{-1} for a mode of wavelength $\lambda = 10 \mu\text{m}$, and of $5 \times 10^4 \text{ sec}^{-1}$ for a mode with $\lambda = 1 \mu\text{m}$.

In the case of F-actin, the predicted amplitude of the high-frequency modulus in Eq. (11) is somewhat higher than experiment. Each actin filament contains fourteen 43-kD monomers per 38-nm half-pitch; it follows that the density of filament length in 1 mg/mL polymerized F-actin is $\rho = 3.8 \times 10^{13} \text{ m}^{-2}$. Using Eq. (11),

$$G(f) \approx (1.6 \text{ Pa}) \left(\frac{c}{1 \text{ mg/mL}} \right) \left(\frac{f}{1 \text{ Hz}} \right)^{3/4} i^{-3/4}. \quad (13)$$

At a concentration of $c = 2$ mg/mL, the imaginary part of Eq. (13) is about seven times larger than an observed power-law modulus of $G''(f) \approx 0.44 \text{ Pa}(f/1 \text{ Hz})^{3/4}$, between 10 and 100 Hz, in Fig. 1B of [5]. We consider this acceptable agreement. The experimental value might be depressed by incomplete polymerization or by a high fraction of short filaments (much shorter than the entanglement length). It is also possible that the persistence length may be shorter without phalloidin present.

The power-law dependence $G(\omega) \propto \omega^{3/4}$ in Eq. (11), is in contrast with well-understood flexible polymer systems that exhibit shear moduli obeying power-laws in the range of $\omega^{1/2}$ to $\omega^{2/3}$ [2]. Identical conclusions to ours have been obtained independently by Morse [10]. This scaling of $G(\omega)$ is in good agreement with prior results of F-actin by microrheology [5] and multiple light scattering [6] experiments, both of which were able to measure the shear modulus at significantly higher frequencies than previously possible for F-actin by conventional rheology. Macroscopic rheology experiments have reported Rouse-like scaling [20], although the range of frequencies (below 3 Hz) may not have been adequate to show the scaling regime above the plateau. Moreover, the experiments of Ref. [20] consistently showed G'' in excess of G' at the highest frequencies, indicating a power-

law greater than $1/2$ [2]. Other microrheology experiments on F -actin [19] have also reported dynamics consistent with $G(\omega) \propto \omega^{3/4}$, although the actin concentrations were lower, and the authors suggested an alternative explanation. As we have noted above, this high-frequency modulus may permit the most direct comparison of experiment with theory in F -actin systems, given the large variation in measured plateau moduli, which may result from the sensitivity to entanglements and crosslinking in semiflexible systems.

We thank D. C. Morse for generous discussions of his related work. We also thank A. C. Maggs, T. Mason, P. D. Olmsted, C. F. Schmidt, B. Schnurr, and D. A. Weitz for many discussions. This work was supported in part by the Whitaker Foundation, the National Science Foundation (Grant Nos. BIR 95-12699 and DMR 92-57544), and by the donors of the Petroleum Research Fund, administered by the ACS. F.C.M. wishes to thank the Aspen Center for Physics.

-
- [1] P.-G. de Gennes, *Scaling Concepts in Polymer Physics* (Cornell University Press, Ithaca, 1979).
- [2] M. Doi and S. F. Edwards, *The Theory of Polymer Dynamics* (Clarendon Press, Oxford, 1988).
- [3] T. Yanagida, M. Nakase, K. Nishiyama, and F. Oosawa, *Nature* (London) **301**, 58 (1984); A. Ott, M. Magasco, A. Simon, and A. Libchaber, *Phys. Rev. E* **48**, R1642 (1993).
- [4] F. Gittes, B. Mickey, J. Nettleton, and J. Howard, *J. Cell Biol.* **120**, 923 (1993).
- [5] F. Gittes, B. Schnurr, P. D. Olmsted, F. C. MacKintosh, and C. F. Schmidt, *Phys. Rev. Lett.* **79**, 3286 (1997); B. Schnurr, F. Gittes, F. C. MacKintosh, and C. F. Schmidt, *Macromolecules* **30**, 7781 (1997).
- [6] T. Giseler and D. A. Weitz, *Mater. Res. Soc. Symp. Proc.* (to be published).
- [7] F. C. MacKintosh, J. Käs, and P. A. Janmey, *Phys. Rev. Lett.* **75**, 4425 (1995).
- [8] K. Kroy and E. Frey, *Phys. Rev. Lett.* **77**, 306 (1995).
- [9] A. C. Maggs, *Phys. Rev. E* **55**, 7396 (1997).
- [10] D. C. Morse, preceding paper, *Phys. Rev. E* **58**, 1237 (1998).
- [11] P. A. Janmey, S. Hvidt, J. Käs, D. Lerche, A. C. Maggs, E. Sackmann, M. Schliwa, and T. P. Stossel, *J. Biol. Chem.* **269**, 32 503 (1994).
- [12] U. Seifert, W. Wintz, and P. Nelson, *Phys. Rev. Lett.* **77**, 5389 (1996).
- [13] R. Granek, *J. Phys. II* **7**, 1761 (1997). This paper independently derives the end-to-end spectrum of a single filament, asymptotically equivalent to our Eq. (8).
- [14] H. Isambert and A. C. Maggs, *Macromolecules* **29**, 1036 (1996).
- [15] Recent experiments by T. Mason (private communication) may have observed a high-frequency regime dominated by simple viscous response. This possibility was also pointed out by A. C. Maggs (private communication).
- [16] F. Gittes and F. C. MacKintosh (unpublished).
- [17] T. Odijk, *Macromolecules* **16**, 1340 (1983); A. N. Semenov, *J. Chem. Soc., Faraday Trans. 2* **82**, 317 (1983).
- [18] J. Lighthill, *Mathematical Biofluidynamics* (Society for Industrial and Applied Mathematics, Philadelphia, 1973).
- [19] F. Amblard, A. C. Maggs, B. Yurke, A. N. Pargellis, and S. Leibler, *Phys. Rev. Lett.* **77**, 4470 (1996).
- [20] O. Müller *et al.*, *Macromolecules* **24**, 3111 (1991); R. Ruddies *et al.*, *Eur. Biophys. J.* **22**, 309 (1993).